Structural Role of Nd2O3 as Dopant Material in Modified Borate Glasses and Glass Ceramics

M. A. Shaalan
faculty of scence mansoura university
Gomaa El-Damrawi (gomaaeldamrawi@gmail.com)
Mansoura University Faculty of Science https://orcid.org/0000-0001-9144-0682
A.K. Hassan
mansoura university
M. Hamed Misbah
Mansoura University

Research Article

Keywords: Bio borate glasses, Neodymium oxide, Micro hardness tester, Crystal phase

Posted Date: February 15th, 2021

DOI: https://doi.org/10.21203/rs.3.rs-194312/v1

Version of Record: A version of this preprint was published at Journal of Materials Science: Materials in Electronics on April 17th, 2021. See the published version at https://doi.org/10.1007/s10854-021-05866-x.

Abstract

Glasses in the system xNd_2O_3-(46-x)B_2O_3-27CaO-24.4Na_2O-2.6 P_2O_5 ($0 \le x \le 4$ mol%) have been prepared via conventional melt quenching technique. X-ray diffraction (XRD) spectra have showed that the amorphous structure is dominant in glasses of Nd_2O_3 concentrations $\le$ 0.5 mol%. But formation of a more ordered structure is confirmed at higher Nd_2O_3 values. Result based on differential scanning calorimetry (DSC) shows an increase in glass transition temperature (T_g) with increasing Nd_2O_3 at expense of B_2O_3 contents. Vicker hardness (H_v) and density (D) are used to correlate the glass structure with its properties. The measured density is found to be increased whereas the molar volume is decreased with increasing Nd_2O_3 content. The calculated molar volume (V_m) and free spaces (V_f) are both decreased due to filling process which is suggested to be carried out by Nd^{3+} of larger size than that of B^{3+}. Decreasing of V_m and V_f can reflect the increase in bridging bonds in the glass network which in turns results in increasing of both T_g and of the investigated compositions.

1. Introduction

A family of rare earth (RE) elements is considered between the elements of the lanthanide group which shows pronounced biological activity as they are capable of replacing Ca^{2+} in investigated glass matrix [1–2]. Most of the recent studies have concentrated on enhancing the bioactivity of glass materials by the effect of RE ions [3–8]. These advances include the preparation of special glass materials, or the introduction of certain useful elements in the matrix of the simple glass materials [9].

The research interest in the branch of borate glass systems is due to their anomalous behavior. Borate glass has been studied most recently in contrast with other traditional glasses due to its good optical and mechanical properties [8, 10]. Borate glass systems are well known to have a stable structure against ambient humidity, good corrosion resistance in mechanical strength and chemical toughness. Borate oxide glasses are one of the most suitable for doping with RE^{3+} ions among the potential host glasses. [8–14].

Due to its high transparently, low melting point, high thermal stability, different coordination numbers and strong solubility of rare-earth ions, borate glass is an especially suitable optical medium [15, 16]. In addition, RE-doped alkali borate glasses are interesting for the study of the effects of alkali ions, especially around rare-earth ions, on the glass forming network. Depending on the type and concentration of the modifier oxide, the addition of an alkali oxide has a strong effect on boron coordination and structural groups [13,17,18,].

In the present work, the properties and structure of some glass ceramics containing Nd_2O_3 have been investigated in terms of its promising features for biomedical applications due to the electronic configuration of Nd_2O_3. Although studies of such glasses have continuously been increasing, they still have been poorly studied as biomaterials. Most current research focuses on improvement the bioactivity of the base glass materials. These improvements include incorporation of some useful elements through the basic glass materials. Also the present work aimed to introduce Nd_2O_3 into the glass matrix in order to research the effects of glass composition on the compatibility and strength of the material, due to the bioactivity effects of the rare earth elements.

2. Materials And Methods

2.1 Preparation of glasses

In the present work, glasses in the system xNd_2O_3-(46-x)B_2O_3-27CaO-24.4Na_2O-2.6 P_2O_5, ($0 \leq x \leq 4$ mol%) have been prepared via conventional melt quenching method. Materials were obtained from mixtures of reagent grade $CaCO_3$, Na_2CO_3, H_3BO_3, Nd_2O_3 and $(NH_4)_2HPO_4$ thoroughly mixed and placed in a Pt-Au crucible. The batches were first heat treated from room temperature to 600 °C with a slow heating rate of 2°/min to remove NH_3 and H_2O and were then melted at 1000-1200 °C during 20-30 min before being quenched by pouring the melt between two metallic plates. Melting time and temperatures were optimized to limit P_2O_5 volatilization and maintain the overall glass weight losses under 2 %.

2.2 XRD measurements

X-Ray diffraction measurements are carried out with Shimadzu X-ray diffract meter (Dx-30, Metallurgy institute, El Tebbin-Cairo). The peak position and intensity values used to identify the type of material were compared with patterns in the international powder diffraction file (PDF) database complied by joint committee for powder diffraction standards (JCPDS).

2.3 Density measurements

By applying Archimedes principle, the densities of the prepared samples were measured with benzene as the immersion liquid. The density was calculated using the formula:

$$\rho = \frac{W_a}{W_a - W_b} \times \rho_b \qquad (1)$$

where, W_a is the weight in air, W_b is the weight in benzene, and P_b is the density of benzene.

2.4. Molar volume calculations

The molar volumes (V_m) were calculated using the equation that follows:

$$V_m = \frac{M_T}{\rho} \qquad (2)$$

in which V_m *is molar volume (cm^3/mol), Mτ is the molecular weight of the glass sample (g/mol) and ρ is the density (g/cm^3) of the sample.*

2.5 Microhardness

The SHIMADZU-HMV-G20S (Shimadzu, Kyoto, Japan), microhardness tester was employed to determine micro hardness number (H_v) of the prepared samples at an ambient temperature under a weight of 50 g and a retention period of 15 s. For certainty of the measurement, ten indentations were taken at different points on the surface of each specific sample. The consequential traces of the indentations were captured and after unloading the corresponding length of the indentation imprint diagonals recorded by a high resolution microscope. The microhardness (Hv) values were calibrated with the help of the formula:

$$H_V = 1.854\ \frac{F}{d^2} \qquad (3)$$

where H_v is Vickers hardness in Hg/mm_2, F is the applied force in newton and d is the mean length of the diagonals of the indentation in meters.

3. Results And Discussion

3.1. XRD spectroscopy

The glasses of low Nd_2O_3 (x =0 and 0.5 mol %). were colorless, transparent and amorphous in nature. The addition of Nd_2O_3 at expense of B_2O_3 has been shown to be very effective in enhancing the crystallization of the glasses. Precipitation of the small sized crystals in the main glass network lowers the sample transparency and the glass in such a case is partially devitrified.

The XRD spectra revealed that an amorphous structure is the characteristic feature of the samples containing $\leq$ 0.5 mol% Nd_2O_3. Transformation into a crystalline structure occurred after introducing higher Nd_2O_3 concentrations. It is shown from figure 1(a, b) that the XRD spectra contains two broad diffraction bands located between 20-30° and 40-55°. Presence of these broaden bands reflects the amorphous structure of the glasses of low Nd_2O_3 concentration (0 and 0.5 mol%). On the other hand, the glasses of higher Nd_2O_3 concentrations become relatively opaque due to formation or precipitation of some crystalline species. Presence of sharp and intense diffraction line plectra in glasses of more Nd_2O_3 content figure 1(c, d, e) can be correlated to formation of the more ordered crystalline phases in the matrix of the investigated materials.

Comparisons between X-ray sharp diffraction line spectra of the studied materials with that of $Ca_3(PO_4)_2$, (CaB_4O_7) and ($NdBO_3$)) crystals were made. It is concluded from the comparison that calcium phosphate, calcium borate and Nd-borate crystalline species are the most formed species. It was found that metaborate (CaB_2O_4) nanoparticles and tetraborate (CaB_4O_7) nanoparticles are the main crystalline phases. In addition, crystalline apatite ($Ca_3(PO_4)_2$) structure is well formed also by the effect of Nd_2O_3 addition.

The diffraction peaks observed at 2 theta values of 23°, 26°, 31.8°, 41.2°, 47°, 48° are belong to calcium tetraborate [ICDD PDF 83-2025]. The XRD peaks at 2 theta values of 23.3°, 24.8°, 28.3°, 32°,47° matching with the (111), (210), (220) and (022) the rhombic structure of calcium meta-borate [ICDD PDF 32-0155].

Figure 2 represents the change of the determined crystallinity with increasing Nd_2O_3 concentration. Then from the figures 1 and 2 one may expect that the crystallization process is offered mainly by effect of Nd_2O_3, since the material containing even limited addition of Nd_2O_3 (> 0.5 mol%) is crystallized. The number of diffraction lines in glasses of 1, 3 and 4 mol% Nd_2O_3 is the same but change in intensities is the most observed parameter. This means that the types of the well-formed crystalline phases are the same but the content of the separated phases increases with increasing Nd_2O_3 concentrations. These modifications are summarized in figure 2, which reflects a change in the structure throughout changes of crystallinity in glass. It can be seen from this figure that with increasing Nd_2O_3 concentration, the crystallinity increases to reach its saturated values in the region between 3 and 4 mol %. This interpretation may account on the presence of several diffraction lines in spectra of glasses modified by more than 0.5 mol% Nd_2O_3 (spectra c, d, e). Some of the well-formed crystalline phases, such as crystalline apatite (calcium phosphate crystals), are categorized as bioactive phases that are useful for the material to be used in the field of biodental and bioactive use [19-26].

There are two parameters that can play a role in improving the process of crystallization in the glasses being tested. The first is the replacement of B_2O_3 with Nd_2O_3, as mentioned above. Secondly, the thermal heat treatment process (THT) is alternatively applied also to improve the crystallization behavior. The latter can be applied on sample containing 4 mol% Nd_2O_3 which characterized with its higher crystallinity in comparison with composition of lower Nd_2O_3. The temperature at which THT process can be considered can be extracted from DSC curves.

3.2 DSC, thermal treatments, glass transition temperature and Vicker hardness

The maximum crystallinity is found in composition of 4 mol% Nd_2O_3 under the effect of glass composition. To assure the stability of the well-formed crystals, the sample of 4 mol% Nd_2O_3 is also investigated under the effect of thermal treated at a specific temperature based on differential scanning ceilometer (DSC) data. As can be shown from figure 3, the DSC curve clearly shows one endothermic peak and one exothermic peak. The endothermic peak corresponds to the glass transition (T_g) while the exothermic peak indicates the crystallization point of the glass (T_c). The glass transition temperature (T_g) as well as crystallization temperature (T_c) are estimated by the slope intercept method. The nature of the DSC curves is typical for other glass compositions. The crystallization temperature was found to be around 800°C. The glass is therefore thermally treated at this temperature. It can be shown from figure 4 that the state of crystallization didn't changes with thermal heat treatment, since XRD spectra of the as prepared and treated samples are nearly not differed. This means that the glass ceramic of 4 mol% Nd_2O_3 is the most recommended composition containing the maximum concentration of crystals.

The thermal analysis of the glasses was carried out because any change in the coordinating number of atom-forming networks or in the formation of non-bridging oxygen (NBO) or bridging bonds (BB) can simply be expressed by the change of T_g with the composition. The variation of T_g with compositions is shown in figure 5. It can be seen that with the rise of Nd_2O_3 content, which is the network intermediate here, T_g increases monotonically. It is documented that with the increase of bridging bonds in the main borate glass network, T_g and crystallization temperature T_c are generally increased [20, 27-30]. It is believed that T_g depends on the strength of chemical bonds in the structure. Nd_2O_3 in general, plays the role of a network intermediate which has been consumed to increase the bonds between different structural units with the increase of its content in the glass system. Increase of bridging oxygen indicates the increase in the strength of chemical bonds, which in turn increases both T_g as shown in figure 5.

3.3 Density, molar volume, free volume and packing density

It was found that the density of glass samples increases with increasing Nd_2O_3 concentration as shown in figure 6. This is due to the higher molecular weight of Nd_2O_3 (336.4822 g/mol) than the host structures of the glass samples (B_2O_3 is 69.6202 g/mol) [19-22]. Therefore, the molar volume (M_v) shows a reverse behavior to density as shown in figure 6. The M_v is the parameter that describes the volume occupied by the unit mass of a glass plus the free volume (V_f) surrounded the structural unit forming the network of the glass. In general, the unit mass is increased upon increasing Nd_2O_3 at the expense of B_2O_3. In addition, the free spaces (V_f) associated with borate or NdO_4 units is decreased as a result of its occupation with Nd^{3+} ions which is of larger size than that of B^{3+}. Then, substitution of B_2O_3 with Nd_2O_3 is therefore decreases the free volume with a manner which depends on the ionic radius of the glass modifier oxide [23]. As a result, increase of density and decrease of free volumes (V_f) are the two factors played the role of decreasing (M_v) of the investigated glasses. The decrease of the molar volume is due to adding Nd^{3+} of larger ionic radius (1.123 Å) into interstitial of host structure as the ionic radius of B^3 is (0.400 Å) lead to reducing the free spaces formed around the structural units. Therefore, substitution of B_2O_3 with Nd_2O_3 decreases the molar volume via reducing the concentration of free spaces which have been filled with Nd^{3+} ions of larges sizes. Decreasing of open spaces with increasing Nd_2O_3 means that the packing density should be increased with decreasing the total molar volume of the glass samples [22-24]. Then increasing P_d (density) and decreasing void spaces in the glass network are considered as the main causes in increasing T_g and H_v of the investigating samples.

4. Conclusions

Nd_2O_3 containing B_2O_3-CaO-Na_2O-P_2O_5 glasses were prepared by conventional melt-quenching technique. The amorphous or crystalline nature of these samples was confirmed by X-ray diffraction (XRD). The calculated crystallinity increases with increasing Nd_2O_3 contents. The measured density, the glass transition temperature T_g and Vicker hardness number are also increased upon Nd_2O_3 addition. The calculated molar volume V_m and free spaces are both decreased due to filling process by Nd^{3+} of larger size than that of B^{3+}. Decreasing of V_m and V_f are the main reasons for increasing the packing density in the glass network.

Declarations

Ethical Statement

Authors declare that we have no conflict of interest. We are agreed upon all the Ethical Rules applicable for this journal.

Declaration of CompetingInterest(No funding)

The authors declare that they have no known competing financial interests or personal relationships that could have appeared to influence the work reported in this paper.

Consent for Publication

Authors asgreed to publish this work in SILICon . This declaration ensures that the Publisher has the Author's permission to publish this work.

Availability of data and materials

As authors, we are increasingly make our research data available and Data will be made available on request.

References

1. 1. Baazm, M.; Soheyli, E.; Hekmatshoar, M.H.; Rostamzad, A.; Abad, A.K.C. Preparation of quaternary boro-phosphate multifunctional glasses and their structural, optical, switching and antibacterial properties. *Ceram. Int.* **2018**, 44(8), 9414-9421, https://doi.org/10.1016/j.ceramint.2018.02.158
2. Thompson, K.H.; Orvig, C. Lanthanide compounds for therapeutic and diagnostic applications. *Chem. Soc. Rev.***2006**, 35(6), 499-499, https://doi.org/ 10.1039/B606622B
3. Baranowska, A.; Kochanowicz, M.; Żmojda, J.; Miluski, P.; Wajda, A.; Leśniak, M.; Dorosz , D. Biological properties of rare-earth doped bioactive glass, Proc. SPIE 11456, Optical Fibers and Their Applications, Bialowieza, Poland, 2020, 11456, pp.1145604. International Society for Optics and Photonics. https://doi.org/10.1117/12.2566347
4. Ershad, M.; Ali, A.; Mehta, N.S. Mechanical and biological response of (CeO_2+La_2O_3)-substituted 45S5 bioactive glasses for biomedical application. *J. Aust. Ceram. Soc.***2020**, (56), 1243–1252, https://doi.org/10.1007/s41779-020-00471-3
5. Amudha, S.; Ramya, J.R.; Arul, K.T.; Deepika, A.; Sathiamurthi, P.; Mohana, B.; Asokan, K.; Dong, C.L.; Kalkura, S.N. Enhanced mechanical and biocompatible properties of strontium ions doped

mesoporous bioactive glass. *Compos. B. Eng.* **2020**, 196, 108099, https://doi.org/10.1016/j.compositesb.2020.108099

6. Pajares-Chamorro, N.; Chatzistavrou. X. Bioactive Glass Nanoparticles for Tissue Regeneration, *ACS Omega* **2020**, 5(22), 12716-12726, https://doi.org/10.1021/acsomega.0c00180
7. Zambannini,T.; Borges, R.; Faria P.C.; Dissolution, bioactivity behavior and cytotoxicity of rare earth containing biopactive glasses (RE=Dd, Yb). *Int. J. Appl. Ceram. Technol.* **2019**, 16(5), pp. 2029-2039, https://doi.org/10.1111/ijac.13317
8. Yang, D.; Pan, Q.; Kang, S.; Dong, G.; Qiu, J. Weakening thermal quenching to enhance luminescence of Er^{3+} doped β-$NaYF_4$ nanocrystals via acid-treatment. *J. Am. Ceram. Soc.* **2019**, 102(10), 6027-6037, https://doi.org/10.1111/jace.16490
9. Hoppe, A.; Güldal, N.S.; Boccaccini, A.R.; A review of the biological response to ionic dissolution products from bioactive glasses and glass-ceramics. *Biomaterials* **2011**, 32(11), 2757-2774, https://doi.org/10.1016/j.biomaterials.2011.01.004
10. Sahar, M.R.; Jehbu, A.K.; Karim, M.M. TeO_2–ZnO–$ZnCl_2$ glasses for IR transmission. *J. Non-Cryst. Solids* **1997**, 213, 164-167, https://doi.org/10.1016/S0022-3093(97)00096-3
11. Lin, H.; Tanabe, S.; Lin, L.; Yang, D.L.; Liu, K.; Wong, W.H.; Yu, J.Y.; Pun, E.Y.B. Infrequent blue and green emission transitions from Eu^{3+} in heavy metal tellurite glasses with low phonon energy. *Phys. Lett. A* **2006**, 358(5-6), 474-477, https://doi.org/10.1016/j.physleta.2006.05.066
12. El-Deen, L.S.; Al Salhi, M.S.; Elkholy, M.M. IR and UV spectral studies for rare earths-doped tellurite glasses. *J. Alloys Compd.* **2008**, 465(1-2), 333-339, https://doi.org/10.1016/j.jallcom.2007.10.104
13. Farouk, M.; Abd El-Maboud, A.; Ibrahim, M.; Ratep, A.; Kashif, I. Optical properties of Lead bismuth borate glasses doped with neodymium oxide. *Spectrochim. Acta A Mol. Biomol. Spectrosc.* **2015**, 149, 338-342, https://doi.org/10.1016/j.saa.2015.04.070
14. Mahamuda, S.; Swapna, K.; Rao, A.S.; Jayasimhadri, M.; Sasikala, T.; Pavani, K.; Moorthy, L.R. Spectroscopic properties and luminescence behavior of Nd^{3+} doped zinc alumino bismuth borate glasses. *J PHYS CHEM SOLIDS* **2013**, 74(9), 1308-1315, https://doi.org/10.1016/j.jpcs.2013.04.009
15. Nanda, K.; Berwal, N.; Kundu, R.S.; Punia, R.; Kishore, N. Effect of doping of Nd^{3+} ions in BaO-TeO_2-B_2O_3 glasses: A vibrational and optical study. *J. Mol. Struct.* **2015**, 1088, 147-154, https://doi.org/10.1016/j.molstruc.2015.02.021
16. Mhareb, M.H.A.; Hashim, S.; Ghoshal, S.K.; Alajerami, Y.S.M.; Saleh, M.A.; Dawaud, R.S.; Razak, N.A.B.; Azizan, S.A.B. Impact of Nd^{3+} ions on physical and optical properties of Lithium Magnesium Borate glass. *Opt. Mater.* **2014**, 37, 391-397, https://doi.org/10.1016/j.optmat.2014.06.033
17. Yano, T.; Kunimine, N.; Shibata, S.; Yamane, M. Structural investigation of sodium borate glasses and melts by Raman spectroscopy. II. Conversion between BO_4 and BO_2O^- units at high temperature. *J. Non-Cryst. Solids* **2003**, 321(3), 147-156, https://doi.org/10.1016/S0022-3093(03)00159-5
18. Rao, A.S.; Ahammed, Y.N.; Reddy, R.R.; Rao, T.R. Spectroscopic studies of Nd^{3+}-doped alkali fluoroborophosphate glasses. *Opt. Mater.* **1998**, 10(4), 245-252, https://doi.org/10.1016/S0925-

3467(97)00055-4

19. El Damrawi, G.; Abdelghany M.A.; Hassan A.K.; Faroun, B. Conductivity and morphological studies on iron borosilicate glasses, *J. Non-Cryst. Solids*, **2020**, 545, 120233, https://doi.org/10.1016/j.jnoncrysol.2020.120233
20. El-Damrawi, G.; Kamal, H.; Doweidar, H.; Dawood, A.E. Microstructure and in vitro bioactivity of metal substituted hydroxyapatite. *Curr. j. appl. sci. technol.* **2016**, 1-12, https://doi.org/10.9734/BJAST/2016/24940
21. Megala, R.; Gowthami, T.; Sushma, N.J.; Kamala, S.; Raju, B.D.P. A study of low threshold and high gain Nd^{3+} ions doped SiO_2-B_2O_3-Na_2CO_3-NaF-CaF_2 glasses for NIR laser applications. *Infrared Phys. Technol.* **2018**, 90, 221-229, https://doi.org/10.1016/j.infrared.2018.03.015
22. Meejitpaisan, P., Phothong, K. and Kaewkhao, J., NIR emission of Nd3+-doped sodium barium borate oxyfluoride glasses for 1.07 m laser materials. *Interdisciplinary Research Review* **2019**, 14(3), 54-59, https://doi.org/ 10.14456/jtir.2019.29
23. Bhatia, B., Meena, S.L., Parihar, V. and Poonia, M., Optical basicity and polarizability of Nd3+-doped bismuth borate glasses. *New Journal of Glass and Ceramics* **2015**, 5(03), 44, https://doi.org/10.4236/njgc.2015.53006
24. Gaikwad, D.K.; Sayyed, M.I.; Botewad, S.N.; Obaid, S.S.; Khattari, Z.Y.; Gawai, U.P.; Afaneh, F.; Shirshat, M.D.; Pawar, P.P. Physical, structural, optical investigation and shielding features of tungsten bismuth tellurite based glasses. *J. Non-Cryst. Solids* **2019**, 503, 158-168, https://doi.org/10.1016/j.jnoncrysol.2018.09.038
25. Kaur, S.; Pandey, O.P.; Jayasankar, C.K.; Chopra, N. Spectroscopic, thermal and structural investigations of Dy^{3+} activated zinc borotellurite glasses and nano-glass-ceramics for white light generation. *J. Non Cryst. Solids* **2019**, 521, 119472, https://doi.org/10.1016/j.jnoncrysol.2019.119472.
26. Martins, A.L.J.; Feitosa, C.A.C.; Santos, W.Q.; Jacinto, C.; Santos, C.C. Influence of BaX_2(X = Cl, F) and Er_2O_3concentration on the physical and optical properties of barium borate glasses. *Phys. B Condensed Matter* **2019**, 558, 146–153, https://doi.org/10.1016/j.physb.2019.01.038.
27. Kaur, S.; Pandey, O.P.; Jayasankar, C.K.; Chopra, N. Spectroscopic, thermal and structural investigations of Dy^{3+} activated zinc borotellurite glasses and nano-glass-ceramics for white light generation. *J. Non-Cryst. Solids* **2019**, 521, 119472, https://doi.org/10.1016/j.jnoncrysol.2019.119472
28. Rani, P.R.; Venkateswarlu, M.; Mahamuda, S.; Swapna, K.; Deopa, N.; Rao, A.S.; Prakash, G.V. Structural, absorption and photoluminescence studies of Sm^{3+} ions doped barium lead alumino fluoro borate glasses for optoelectronic device applications. *Mater. Res. Bull.* **2019**, 110, 159-168, https://doi.org/10.1016/j.materresbull.2018.10.033
29. Zaman, F.; Rooh, G.; Srisittipokakun, N.; Ahmad, T.; Khan, I.; Shoaib, M.; Rajagukguk, J.; Kaewkhao, J. Comparative investigations of gadolinium based borate glasses doped with Dy^{3+} for white light

generations. *Solid State Sci.* **2019**, 89, 50-56, https://doi.org/10.1016/j.solidstatesciences.2018.12.020

30. Khan, I.; Rooh, G.; Rajaramakrishna, R.; Srisittipokakun, N.; Wongdeeying, C.; Kiwsakunkran, N.; Wantana, N.; Kim, H.J.; Kaewkhao, J.; Tuscharoen, S. Photoluminescence and white light generation of Dy_2O_3 doped Li_2O-BaO-Gd_2O_3-SiO_2 for white light LED. *J. Alloys Compd.* **2019**, 774, 244-254, https://doi.org/10.1016/j.jallcom.2018.09.156

Figures

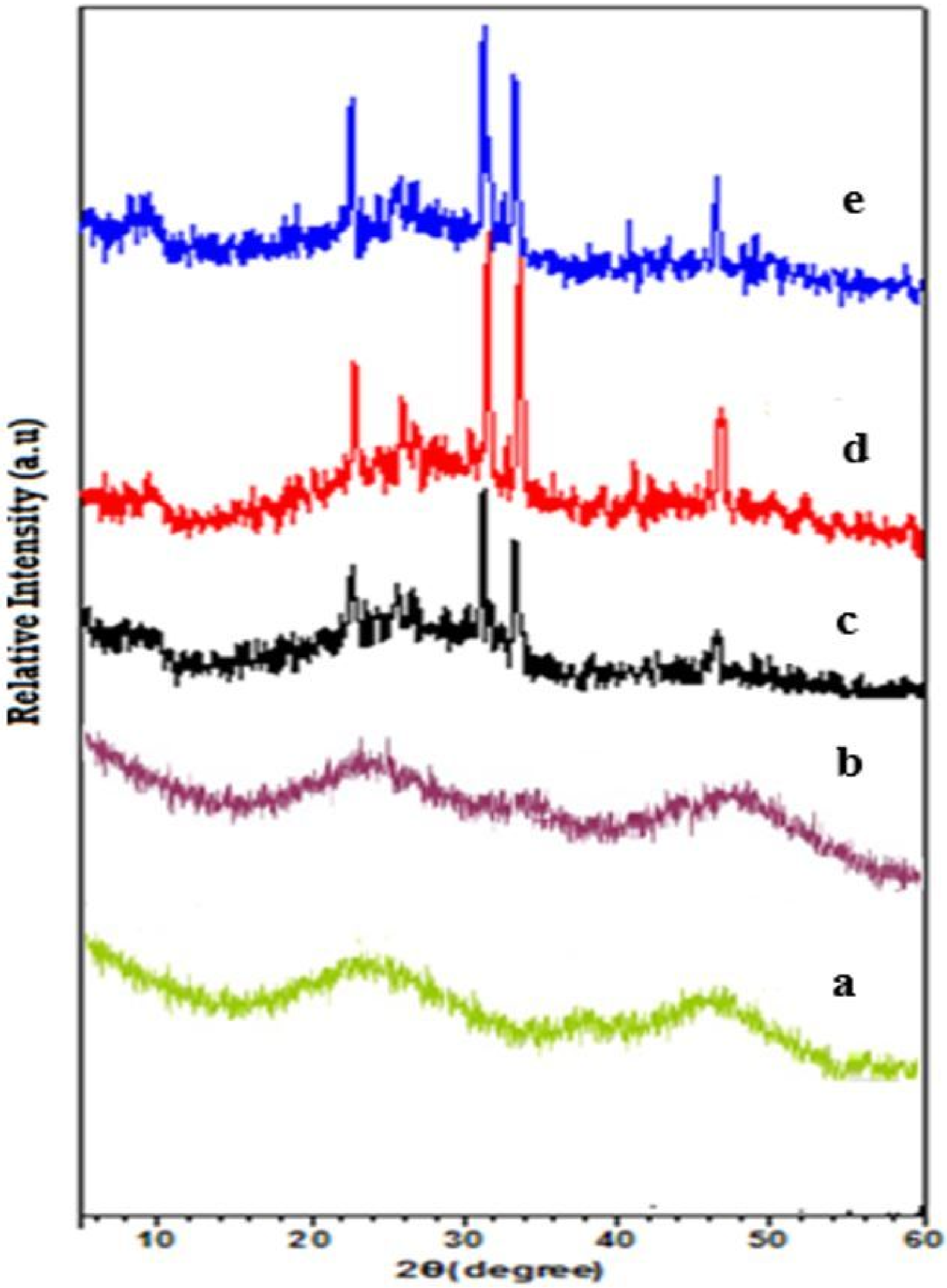

Figure 1

The X-ray diffraction (XRD) patterns of borate glasses containing different Nd2O3 concentrations. The amorphous structure is dominant in glasses of Nd2O3 concentration ≤ 0.5 mol% Nd2O3 spectra (a, b) and crystalline structure is the characteristic feature of glasses of higher Nd2O3 concentrations (c, d, e).

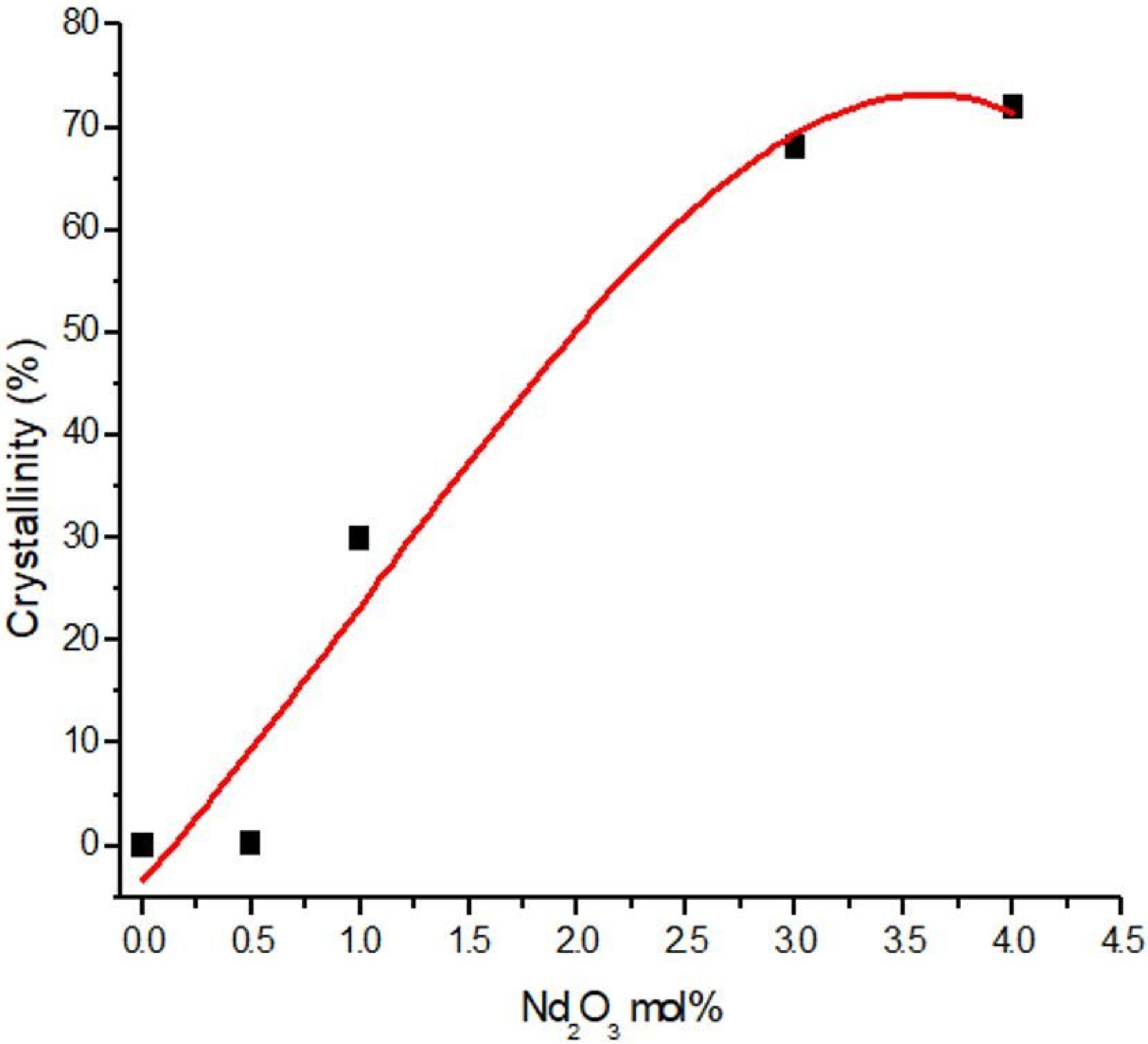

Figure 2

The changes of crystallization process depending on the concentration of Nd2O3.

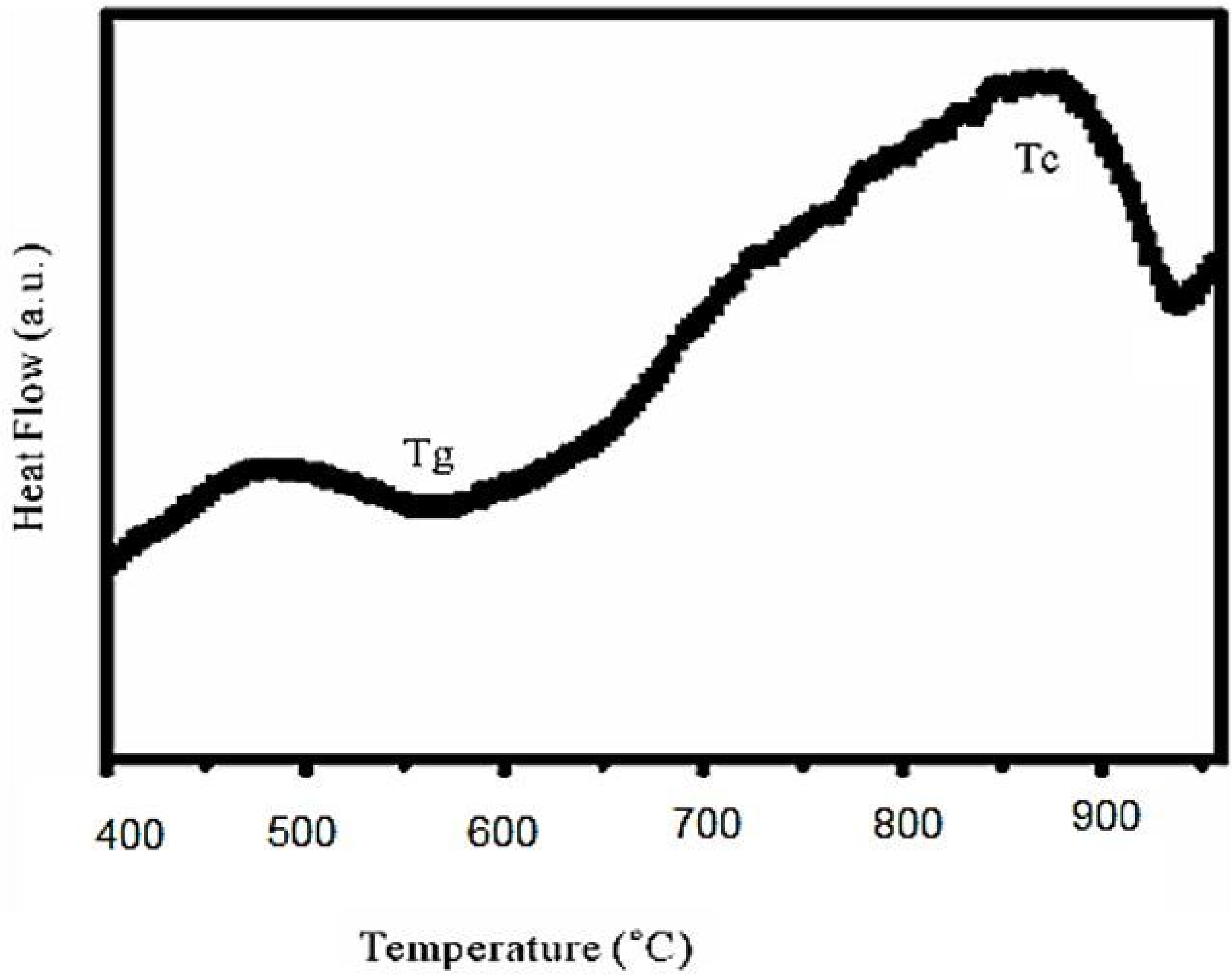

Figure 3

Differential scanning calorimetric curve of 4 mol% Nd2O3 glass.

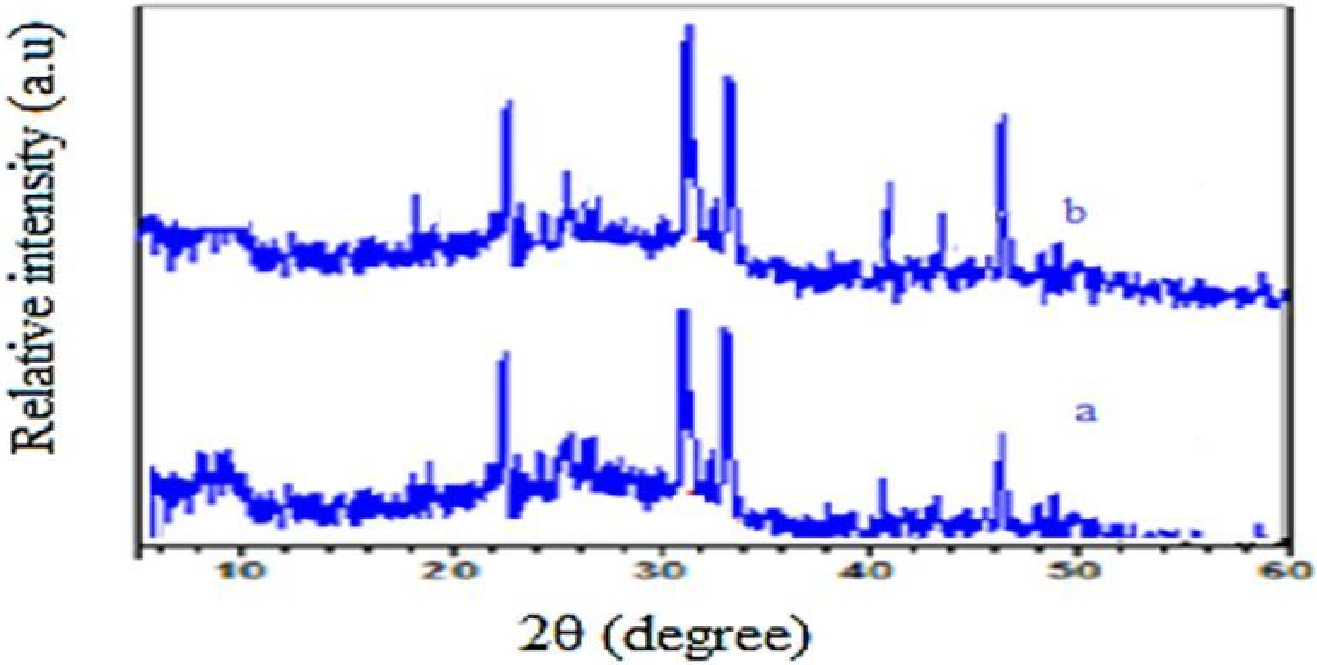

Figure 4

The X-ray diffraction (XRD) patterns glass of 4 mol% Nd2O3 (a) as prepared and (b) thermally treated.

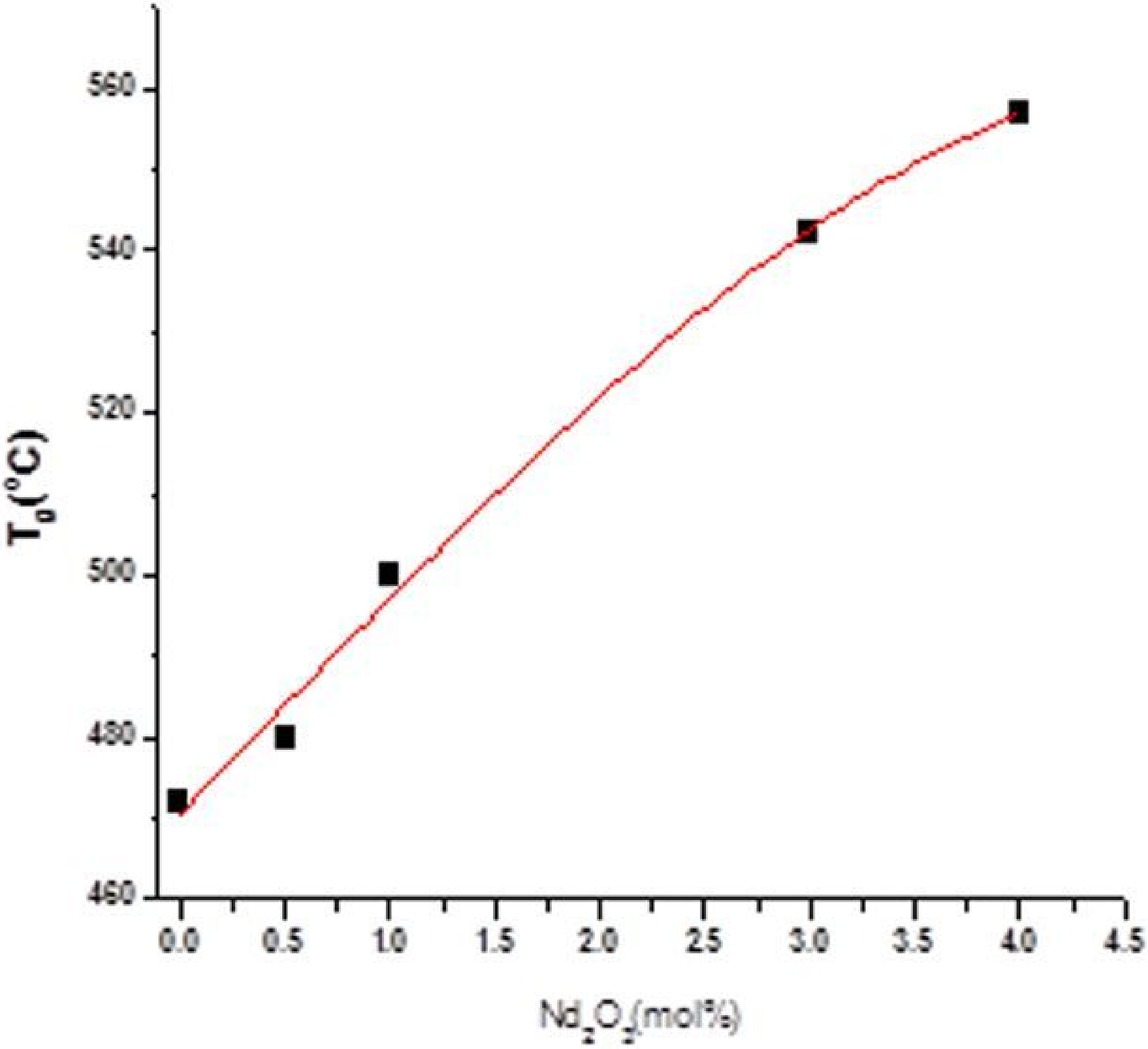

Figure 5

The variation of Tg with Nd2O3 concentration.

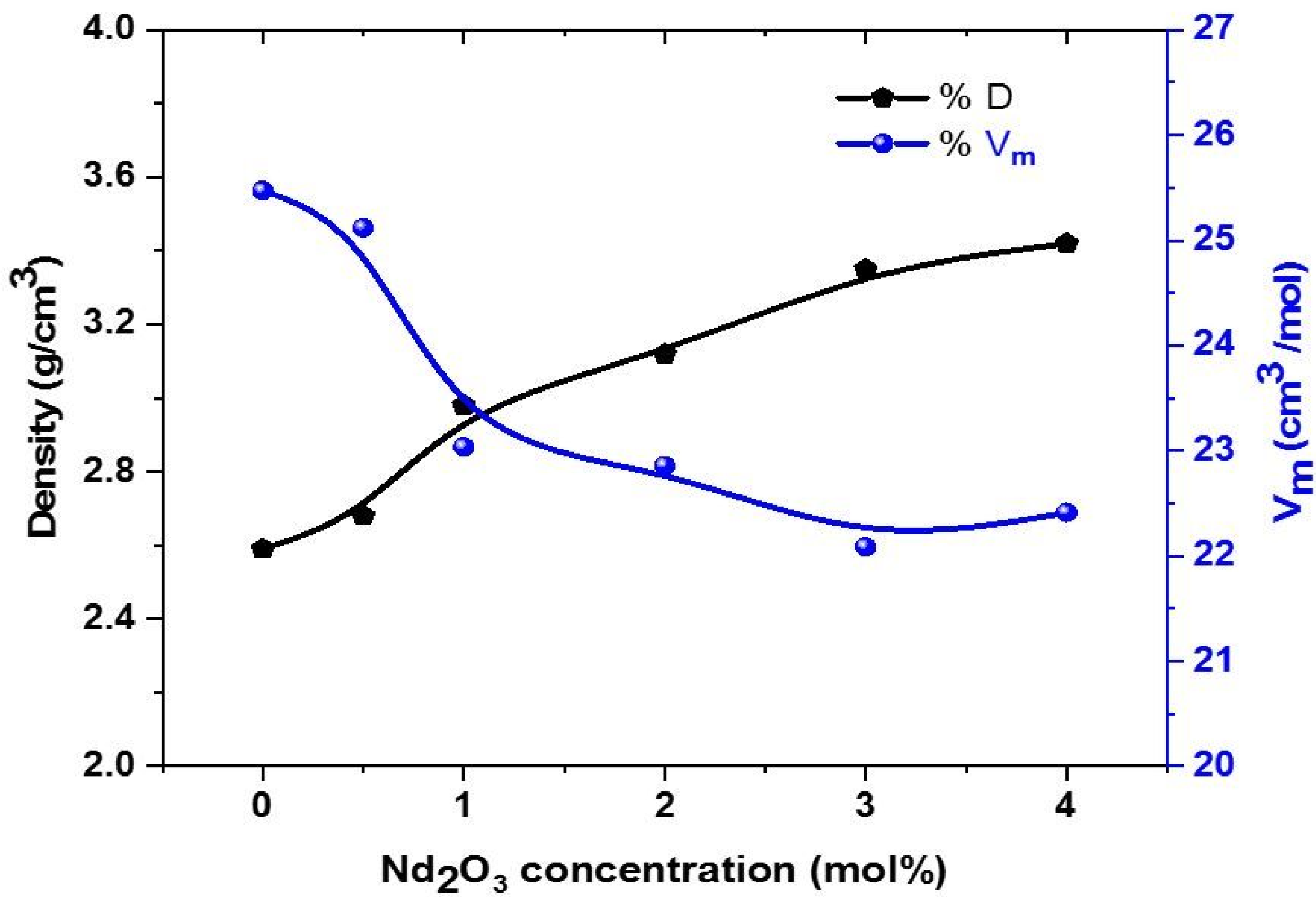

Figure 6

Density and molar volume versus to Nd2O3 concentration.

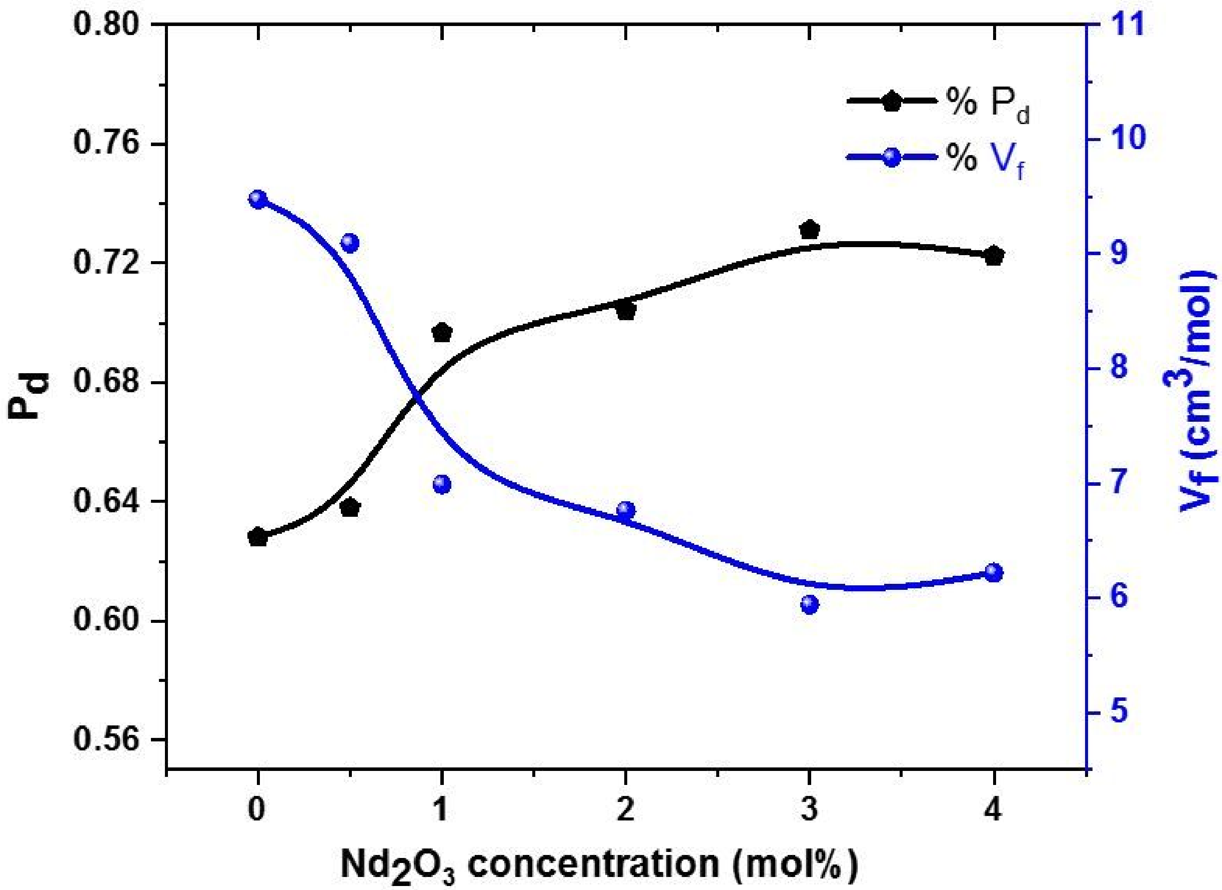

Figure 7

Packing density and free volume versus to Nd2O3 concentration.